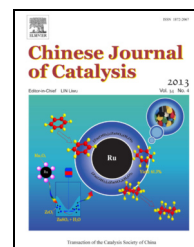


available at www.sciencedirect.comjournal homepage: www.elsevier.com/locate/chnjc

Article

Selective hydrogenation of benzene to cyclohexene over nanocomposite Ru-Mn/ZrO₂ catalysts

SUN Haijie, JIANG Houbing, LI Shuaihui, WANG Hongxia, PAN Yajie, DONG Yingying, LIU Shouchang, LIU Zhongyi*

College of Chemistry and Molecular Engineering, Zhengzhou University, Zhengzhou 450001, Henan, China

ARTICLE INFO

Article history:

Received 10 October 2012

Accepted 20 November 2012

Published 20 April 2013

Keywords:

Benzene

Selective hydrogenation

Cyclohexene

Ruthenium

Manganese

Zirconia

Zinc

ABSTRACT

A series of Ru-Mn catalysts with different Mn contents were prepared by coprecipitation, and their catalytic performance, using nanoscale ZrO₂ as a dispersant, for the selective hydrogenation of benzene to cyclohexene was investigated. The catalysts were characterized using X-ray diffraction, transmission electron microscopy, N₂ physisorption, X-ray fluorescence, atomic absorption spectroscopy, and Auger electron spectroscopy. The results confirmed that the Mn existed as Mn₃O₄ on the Ru surface. The Mn₃O₄ reacted with ZnSO₄ to form an insoluble [Zn(OH)₂]₃(ZnSO₄)(H₂O)₃ salt, which was readily chemisorbed on the Ru surface. This chemisorbed salt played a key role in improving the cyclohexene selectivity over the Ru catalyst. The cyclohexene yield of 61.3% was obtained over the Ru-Mn catalyst with the optimum Mn content of 5.4%. This catalyst had good stability and excellent reusability.

© 2013, Dalian Institute of Chemical Physics, Chinese Academy of Sciences.

Published by Elsevier B.V. All rights reserved.

1. Introduction

The production of nylon-6 and nylon-66 from benzene and cyclohexene has attracted much attention because it is a safe, environmentally benign, and atomic economic process [1–4]. Hydrogenation of benzene to cyclohexene is thermodynamically favored [5]. The development of a catalyst with high cyclohexene selectivity in the hydrogenation of benzene is therefore important for this technology.

Second metals or metal oxides could significantly improve the cyclohexene selectivities and yields of Ru-based catalysts. Xie et al. [6] prepared an Ru-B/SiO₂ catalyst by impregnation and chemical reduction methods, and found that the activity and cyclohexene selectivity of this catalyst in H₂ reduction of

benzene were better than those of an Ru/SiO₂ catalyst with the same Ru loading. They also revealed that the B was present in two forms, namely oxidized and elemental B species, and modification of their hydrophilicities on the surface of the Ru-B/SiO₂ catalyst gave this catalyst high activity and high cyclohexene selectivity. Liu et al. [7] prepared an Ru-La-B/ZrO₂ catalyst using a chemical reduction method and obtained a cyclohexene yield of 53.2% and a corresponding cyclohexene selectivity of 61.9%. They confirmed that the La in this catalyst existed as La₂O₃. Fan et al. [8] prepared an Ru-Co-B/γ-Al₂O₃ catalyst using an impregnation reduction method, and achieved a cyclohexene yield of 28.8% without any additives. They discovered that the Co in this catalyst was present as an oxide. Liu et al. [9] prepared an Ru-Ce/SBA-15 catalyst using a “two-solvent” im-

*Corresponding author. Tel: +86-371-67783384; E-mail: liuzhongyi@zzu.edu.cn

This work was supported by the National Nature Science Foundation of China (21273205), the Innovation Found for Technology Based Firms of China (10C26214104505), the China Postdoctoral Science Foundation (2012M511125), and the Scientific Research Foundation of Graduate School of Zhengzhou University.

DOI: 10.1016/S1872-2067(11)60489-0 | <http://www.sciencedirect.com/science/journal/18722067> | Chin. J. Catal., Vol. 34, No. 4, April 2013

pregnation method and achieved a cyclohexene yield of 53.8% over the catalyst with an optimum Ce/Ru molar ratio of 0.25. They found that the Ce existed as a Ce(III) species. These studies provide a good basis for the development of catalysts and catalytic systems for the selective hydrogenation of benzene to cyclohexene.

In previous work, we developed nano-amorphous Ru-M-B/ZrO₂ (M = Zn, Co, Fe, La) catalysts with Ru loadings less than one-third those of industrial Ru-Zn catalysts and obtained a cyclohexene selectivity of 78.8% at a benzene conversion of 59.6%. This was much better than the cyclohexene selectivity of 80% at a benzene conversion of 40% obtained over industrial Ru-Zn catalysts [10–12]. We developed monolayer dispersed Ru-Si-M (M = Zn, Mn, Fe, Ce, La) catalysts and achieved a cyclohexene selectivity of 80% at a benzene conversion of 60%. The catalysts were used in a commercial unit and were shown to be economical, safe, and environmentally friendly. We have applied for national patents for these catalysts [13,14]. In this work, we prepared a series of Ru-Mn catalysts with different Mn contents, investigated the influence of different Mn contents on the performance of the Ru catalysts in selective hydrogenation of benzene to cyclohexene, and determined the role of the Mn promoter. The stability and reusability of the Ru-Mn/ZrO₂ catalyst with an optimum Mn content of 5.4% were also investigated.

2. Experimental

2.1. Catalyst preparation

RuCl₃·H₂O (9.75 g) and the desired amount of MnSO₄·H₂O were dissolved in 200 ml of H₂O with agitation. A 10% NaOH solution was added to the stirred solution. After the reaction was complete, the mixture was filtrated and the black precipitate was washed three times with distilled water. This black precipitate was then dispersed in 400 ml of a 5% NaOH solution and charged in a 1-L Teflon-lined autoclave. The reduction conditions were as follows: H₂ pressure 5 MPa, temperature 150 °C, stirring rate 800 r/min, and time 3 h. The obtained black powder was washed with distilled water until neutrality was achieved, and subsequently vacuum-dried, giving the desired Ru-Mn catalyst. The catalyst was divided into two portions. One portion was used for activity tests and the other was used for catalyst characterization. This ensured the catalysts with different Mn contents had the same Ru contents. The amounts of MnSO₄·H₂O were adjusted to give catalysts with different Mn contents, denoted by Ru-Mn(*x*), where *x* denotes the weight percentage of Mn in the catalyst, determined by atomic absorption spectrometry. Ru-Mn catalysts prepared using different Mn precursors were obtained according to the above procedure, except that MnSO₄·H₂O was replaced by equal molar amounts of Mn(NO₃)₂ or MnCl₂.

2.2. Catalyst characterization

The weight percentages of Mn and the concentration of Mn²⁺ and Zn²⁺ were analyzed by inductively coupled plas-

ma-atomic emission spectroscopy (ICP-AES) on an ICAT 6000 SERIES instrument of Heme Electron corporation. X-ray diffraction (XRD) patterns were acquired using a PANalytical X'Pert PRO instrument with Cu K_α (λ = 0.1541 nm) radiation and a scan range of 2θ = 5°–90° in steps of 0.03°. Transmission electron microscopy (TEM) was performed using a JEOL JEM-2100 instrument. N₂ physisorption (Brunauer-Emmett-Teller method) was determined using a Quantachrome Nova 100e apparatus. The compositions of the catalysts were determined by X-ray fluorescence (XRF), using a Bruker S4 Pioneer instrument. Auger electron spectroscopy (AES) of the Zn LMM transitions was performed using a ULVAC PHI-700 nanoscanning Auger system with an on-axis scanning Ar-ion gun and a cylindrical mirror energy analyzer. The energy resolution was 0.1%. The background pressure of the analysis room was less than 5.2 × 10⁻⁷ Pa. The standard sample was SiO₂/Si.

2.3. Activity tests

The selective hydrogenation of benzene was performed in a 1-L Hastelloy-lined autoclave. A sample of Ru-Mn catalyst, 9.8 g of ZrO₂, and 49.2 g of ZnSO₄ were charged in the autoclave. Heating was begun with an H₂ pressure of 5 MPa and a stirring rate of 800 r/min. Benzene (140 ml) was fed into the system and the stirring rate was increased to 1400 r/min to prevent diffusion effects when the temperature reached 150 °C. The reaction process was monitored by taking small samples of the reaction mixture every 5 min. The products were analyzed by gas chromatography using a GC-1690 gas chromatograph with a flame ionization detector (Hangzhou Kexiao Instrument Co., China). The benzene conversion and cyclohexene selectivity were calculated from the product concentration obtained using corrected peak area normalization. At the end of the reaction, the organic phase was removed using a separating funnel. The slurry containing the mixture of the catalyst and ZrO₂ was reused, according to the above operations, without any additions. The catalysts after hydrogenation were denoted by Ru-Mn(*x*)/ZrO₂, where *x* is the weight percentage of Mn in the catalyst, determined by atomic absorption spectrometry. The Ru-Mn(5.4%) catalyst without the addition of ZrO₂ after hydrogenation was denoted by Ru-Mn(5.4%) AH, where AH represents after hydrogenation.

3. Results and discussion

3.1. Catalyst characterization results

Figure 1 shows the XRD patterns of the Ru-Mn(*x*) catalysts and the Ru-Mn(*x*) catalysts with ZrO₂ as a dispersant after hydrogenation. Figure 1(a) shows that all the Ru-Mn(*x*) catalysts display the diffraction peaks of the hexagonal phases of metallic Ru (JCPDS 01-070-0274) at 2θ = 38.5°, 42.3°, 44.0°, 58.3°, 69.2°, 78.4°, and 38.5°. The Ru-Mn(8.0%) and Ru-Mn(10.8%) catalysts show the diffraction peaks of Mn₃O₄ (JCPDS 00-001-1127) at 2θ = 18.0°, 32.7°, 36.1°, 58.9°, and 69.3°. Morales et al. [15] confirmed that the Mn in a Co-Mn/TiO₂ catalyst reduced below

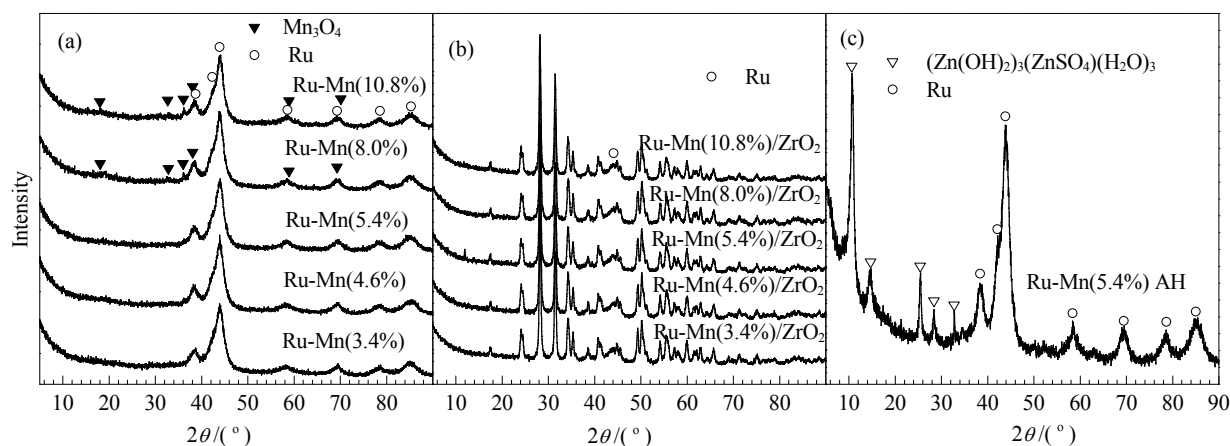


Fig. 1. XRD patterns of Ru-Mn(*x*) (a), Ru-Mn(*x*)/ZrO₂ (b), and Ru-Mn(5.4%) AH (c) samples. Ru-Mn(*x*) denotes Ru-Mn catalysts, where *x* is the mass percentage of Mn in the catalyst; Ru-Mn(*x*)/ZrO₂ is Ru-Mn(*x*) catalyst with ZrO₂ as a dispersant after hydrogenation; Ru-Mn(*x*) AH is Ru-Mn(*x*) catalyst without ZrO₂ after hydrogenation.

Table 1

Textural properties and crystallite sizes of Ru-Mn(*x*) catalysts.

Catalyst	Surface area (m ² /g)	Pore diameter (nm)	Pore volume (ml/g)	Crystallite size (nm)
Ru-Mn(3.4%)	72	12.2	0.22	3.7
Ru-Mn(4.6%)	71	11.8	0.21	4.3
Ru-Mn(5.4%)	62	11.6	0.18	3.8
Ru-Mn(8.0%)	68	9.4	0.16	4.0
Ru-Mn(10.8%)	56	11.2	0.16	4.5

300 °C existed as Mn₃O₄. The reduction temperature was only 150 °C. These results prompted us to suggest that the Mn in the Ru-Mn(*x*) catalysts was mainly present as Mn₃O₄. When the Mn

contents were in the range 3.4%–5.4%, the diffraction peaks of Mn₃O₄ were not observed in the XRD patterns of the Ru-Mn(*x*) catalysts as a result of the low amounts and small crystallites of Mn₃O₄.

Table 1 presents the Ru crystallite sizes of the catalysts calculated from the strongest peak broadening at $2\theta = 44^\circ$ using the Scherrer equation. As can be seen, the Ru crystallite sizes of the Ru-Mn(*x*) catalysts were distributed in the narrow range 3.7–4.5 nm, indicating that the introduction of Mn₃O₄ had little effect on the Ru crystallite sizes.

Figure 1(b) shows that all the Ru-Mn(*x*)/ZrO₂ catalysts after hydrogenation have the weak diffraction peaks of metallic Ru at $2\theta = 44.0^\circ$, indicating small Ru crystallite sizes. All the other

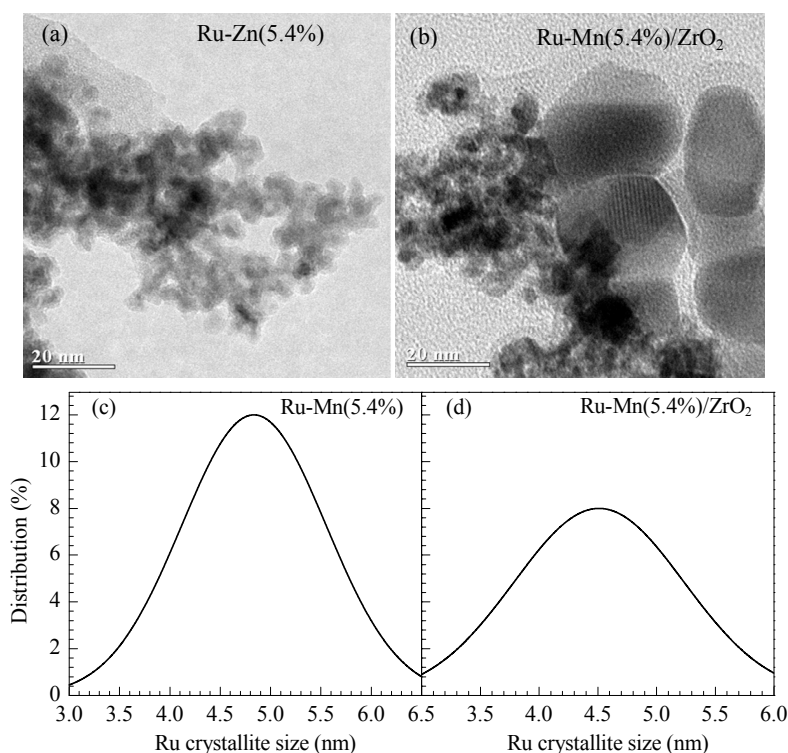


Fig. 2. TEM images (a, b) and Ru crystallite size distributions (c, d) of Ru-Mn(5.4%) and Ru-Mn(5.4%)/ZrO₂.

diffraction peaks corresponded to the monoclinic phases of ZrO_2 (JCPDS 00-024-1165). Figure 1(c) shows that the Ru-Zn(5.4%) catalyst without the addition of ZrO_2 after hydrogenation displayed not only the diffraction peaks of metallic Ru but also the diffraction peaks of the $[\text{Zn}(\text{OH})_2]_3(\text{ZnSO}_4)(\text{H}_2\text{O})_3$ salt (JCPDS 01-078-0247). This indicated that the $[\text{Zn}(\text{OH})_2]_3(\text{ZnSO}_4)(\text{H}_2\text{O})_3$ salt had formed on the surface of the Ru-Mn(5.4%) catalyst after hydrogenation in the presence of ZnSO_4 . However, the diffraction peaks of this salt were not observed on the surface of the Ru-Mn(x) catalysts after hydrogenation with the addition of ZrO_2 , suggesting that this salt was highly dispersed on the surface of the Ru-Mn(x) catalysts and the ZrO_2 dispersant. Xie et al. [16] confirmed that many salts could spontaneously disperse on the support surfaces.

Figure 2 shows the TEM images of the Ru-Mn(5.4%) catalyst and the Ru-Mn(5.4%) catalyst after hydrogenation, with ZrO_2 as a dispersant, and the corresponding Ru crystallite size distributions. Figure 2(a) shows that the Ru-Mn(5.4%) catalyst consisted of nanoscale spherical and ellipsoidal Ru crystallites. Figure 2(c) shows that the Ru crystallite size of the Ru-Mn(5.4%) catalyst was concentrated at around 4.8 nm, which was consistent with the XRD results. Figure 2 shows that the ZrO_2 dispersant mainly consisted of ZrO_2 crystallites of size about 20 nm. The catalyst particles were separated and isolated by ZrO_2 after the first hydrogenation, indicating that a suitable amount of ZrO_2 could significantly suppress agglomeration, which could have occurred as a result of collisions among different catalyst particles under high agitation [17]. Figure 2(d) shows that the Ru crystallite sizes of the Ru-Mn(5.4%)/ ZrO_2 catalyst after hydrogenation were mainly distributed at around 4.5 nm, which is much smaller than the crystallites of the Ru-Mn(5.4%) catalyst before hydrogenation. This indicated that the ZrO_2 played an important role in dispersing the catalyst particles.

Table 1 shows the textural properties of the Ru-Mn(x) catalysts. As can be seen, the surface areas, pore volumes, and pore diameters generally decreased with the Mn content of the catalysts. Zhang et al. [18] found that the specific surface area of a Co-Mn/ TiO_2 catalyst was less than that of TiO_2 , and they suggested that amorphous MnO_x was dispersed on the TiO_2 surface and blocked some of the catalyst pores. Similarly, it is proposed that Mn_3O_4 was dispersed on the surface of the catalysts and could block some of the catalyst pores, resulting in decreases in

the surface areas, pore volumes, and pore diameters. The textural properties of the Ru-Mn(x) catalysts after hydrogenation were similar to that of ZrO_2 because the mass ratio of ZrO_2 to catalyst was 5:1 [19]. N_2 physisorption studies of the Ru-Mn(x)/ ZrO_2 after hydrogenation were therefore not necessary.

Table 2 shows the compositions of the Ru-Mn(x)/ ZrO_2 and Ru-Mn(x) AH, the concentrations of metallic ions in the aqueous phase, and the pH values of the aqueous phase at room temperature. The Mn/Ru, Zn/Ru, and Zr/Ru atomic ratios clearly reflect the variations in the catalyst compositions before and after hydrogenation. Ru-Mn(x) catalysts with different Mn contents were prepared using $\text{MnSO}_4\cdot\text{H}_2\text{O}$ as the precursor. As can be seen from Table 2, the molar ratios of the Ru-Mn(x)/ ZrO_2 catalysts after hydrogenation were all 0.02, indicating trace amounts of Mn in the Ru-Mn(x)/ ZrO_2 after hydrogenation. The Zn/Ru atomic ratios of Ru-Mn(x)/ ZrO_2 after hydrogenation increased, and the concentrations of Mn^{2+} in the aqueous phase increased and the concentrations of Zn^{2+} decreased with Mn content. In particular, the colorless slurries after hydrogenation prompted us to propose that the Mn in the slurries existed as Mn^{2+} . All of these results indicated that the Mn_3O_4 on the surfaces of the Ru-Mn(x) catalysts had reacted with ZnSO_4 to form a new Zn species and an Mn(II) species. The Zn species were chemisorbed on the Ru surfaces and the Mn(II) species were dissolved in the slurries. A trace amount of Mn was also detectable in the Ru-Mn(5.4%) catalyst without the addition of ZrO_2 after hydrogenation. Its Zn/Ru molar ratio was similar to that with ZrO_2 . It was also found that the S/Ru molar ratio for the catalyst without ZrO_2 was 0.06, which was consistent with the XRD results, and showed that the Zn species existed as the $[\text{Zn}(\text{OH})_2]_3(\text{ZnSO}_4)(\text{H}_2\text{O})_3$ salt. The addition of ZrO_2 lowered the S contents of the Ru-Mn(x) catalysts after hydrogenation to below the detection limit of the XRF instrument. All these results implied that the Zn species existed as the $[\text{Zn}(\text{OH})_2]_3(\text{ZnSO}_4)(\text{H}_2\text{O})_3$ salt. The amount of $[\text{Zn}(\text{OH})_2]_3(\text{ZnSO}_4)(\text{H}_2\text{O})_3$ salt increased with the Mn_3O_4 content, which resulted in an increase in the Zn/Ru atomic ratio. It was concluded that the Mn_3O_4 was mainly present on the Ru surface because the ZnSO_4 in the slurry could only react with Mn_3O_4 on the Ru surface, i.e., the $[\text{Zn}(\text{OH})_2]_3(\text{ZnSO}_4)(\text{H}_2\text{O})_3$ salt formed could only be chemisorbed on the Ru surface. Table 2 shows that the pH values of the aqueous solutions after hydro-

Table 2

Composition of Ru-Mn(x)/ ZrO_2 catalysts after hydrogenation and concentrations of the metallic ions in the aqueous phase as well as their pH values at room temperature.

Sample	Mn source	Elemental ratio ^a (mol/mol)			Ion concentration ^b (mol/L)		pH value ^c
		Mn/Ru	Zn/Ru	Zr/Ru	Zn^{2+}	Mn^{2+}	
Ru-Mn(3.4%)/ ZrO_2	MnSO_4	0.02	0.34	5.16	0.44	3.11×10^{-3}	5.6
Ru-Mn(4.6%)/ ZrO_2	MnSO_4	0.02	0.42	5.12	0.43	4.11×10^{-3}	5.4
Ru-Mn(5.4%)/ ZrO_2	MnSO_4	0.02	0.46	4.98	0.42	6.36×10^{-3}	6.0
Ru-Mn(8.0%)/ ZrO_2	MnSO_4	0.02	0.52	5.07	0.41	9.82×10^{-3}	5.9
Ru-Mn(10.8%)/ ZrO_2	MnSO_4	0.02	0.55	5.26	0.37	1.0×10^{-2}	6.2
Ru-Mn(5.2%)/ ZrO_2	$\text{Mn}(\text{NO}_3)_2$	0.01	0.45	5.04	—	—	—
Ru-Mn(5.6%)/ ZrO_2	MnCl_2	0.02	0.47	5.17	—	—	—
Ru-Mn(5.4%) AH	MnSO_4	0.02	0.49	0	—	—	6.0

^a Measured by X-ray fluorescence (XRF).

^b Determined by ICP-AES.

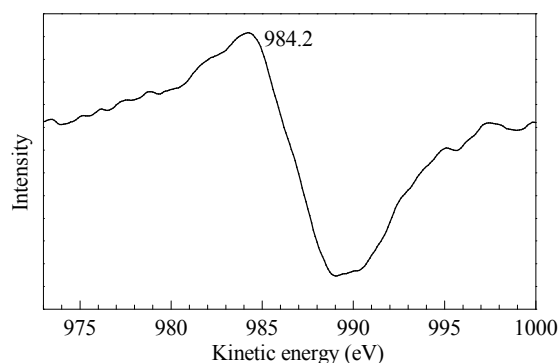


Fig. 3. AES Zn LMM spectrum of Ru-Mn(5.4%)/ZrO₂ sample.

generation generally increased with Mn content of the catalyst. More Mn₃O₄ reacted with more ZnSO₄ to form the [Zn(OH)₂]₃(ZnSO₄)(H₂O)₃ salt, resulting in a decrease in the Zn²⁺ concentrations. The degree of hydrolysis of ZnSO₄ therefore decreased and the pH values of the aqueous solutions increased. The molar ratios of the Ru-Mn(x)/ZrO₂ catalysts after hydrogenation were stable, at around 5.00, as a result of the fixed amounts of ZrO₂.

Ru-Mn(x) catalysts were prepared from different precursors, namely MnSO₄, Mn(NO₃)₂, and MnCl₂, in equimolar quantities. The Mn mass percentages in the catalysts, measured by atomic absorption spectroscopy, were 5.4%, 5.2%, and 5.6%, respectively. Table 2 shows that the Mn/Ru, Zn/Ru, and Zr/Ru atomic ratios of the Ru-Mn(x)/ZrO₂ catalysts after hydrogenation were similar, indicating similar chemical compositions of the Ru-Mn(x)/ZrO₂ catalysts after hydrogenation.

The Zn(II) species chemisorbed on the Ru surface played an important role in improving the cyclohexene selectivities of the Ru catalysts [20–23]. However, there are different opinions about the Zn valence. Wang et al. [20] characterized Ru-Zn/m-ZrO₂ catalysts using XPS and found that the Zn 2p_{3/2} binding energy (BE) of the Zn in the catalyst was close to that of metallic Zn. They suggested that chemisorbed Zn²⁺ cations

could be reduced to metallic Zn by the hydrogen atoms that spilled from the surface of the Ru catalyst. Yuan et al. [21] and He et al. [22] also indicated that Zn atoms could be introduced into Ru-based catalysts by the reduction of Zn²⁺, based on XPS results. However, Struijk et al. [24] indicated that the Zn²⁺ in the adsorption of ZnSO₄ could not be reduced on the surface of an Ru catalyst, also on the basis of XPS results. An important reason for such differences is the closeness of the Zn 2p_{3/2} BEs corresponding to Zn(II) and metallic Zn. It is therefore very difficult to assess the valences of Zn based on the Zn 2p_{3/2} BEs [25]. This drawback can be overcome by using the Zn LMM Auger transition, as the Auger shift between Zn(II) and metallic Zn is higher than 4.6 eV [26]. Figure 3 shows the AES Zn LMM spectra of the Ru-Mn(5.4%) catalyst with ZrO₂ after hydrogenation. The spectra were recorded after Ar⁺ sputtering for 1 min to avoid interruptions of the surface oxidation of the catalyst. As can be seen, the kinetic energy of Zn LMM for Ru-Mn(5.4%)/ZrO₂ after hydrogenation was 984.2 eV, which was in agreement with that of Zn(II) species [27,28]. This was also consistent with the XRD result that the Zn species existed as the [Zn(OH)₂]₃(ZnSO₄)(H₂O)₃ salt. This also indicates that the Zn species chemisorbed on the Ru surface were still present as Zn²⁺ even under reaction conditions of 150 °C and an H₂ pressure of 5.0 MPa. The AES measurements did not identify any additional contributions from metallic Zn (commonly appearing in the 991–995 eV range), indicating that the Zn²⁺ chemisorbed on the Ru surface could not be reduced to metallic Zn. The results in Table 2 show that the aqueous solutions after hydrogenation at room temperature were acidic, as a result of the hydrolysis of ZnSO₄. It is well known that higher temperatures favor hydrolysis. This means that the acidity of the liquid phase is much higher at a reaction temperature of 150 °C as a result of the increase in the degree of hydrolysis of ZnSO₄. As is known, it is difficult for metallic Zn to exist in acidic solutions, and this is consistent with there being no clear evidence in the AES results of the presence of metallic Zn on the surface of the Ru catalysts.

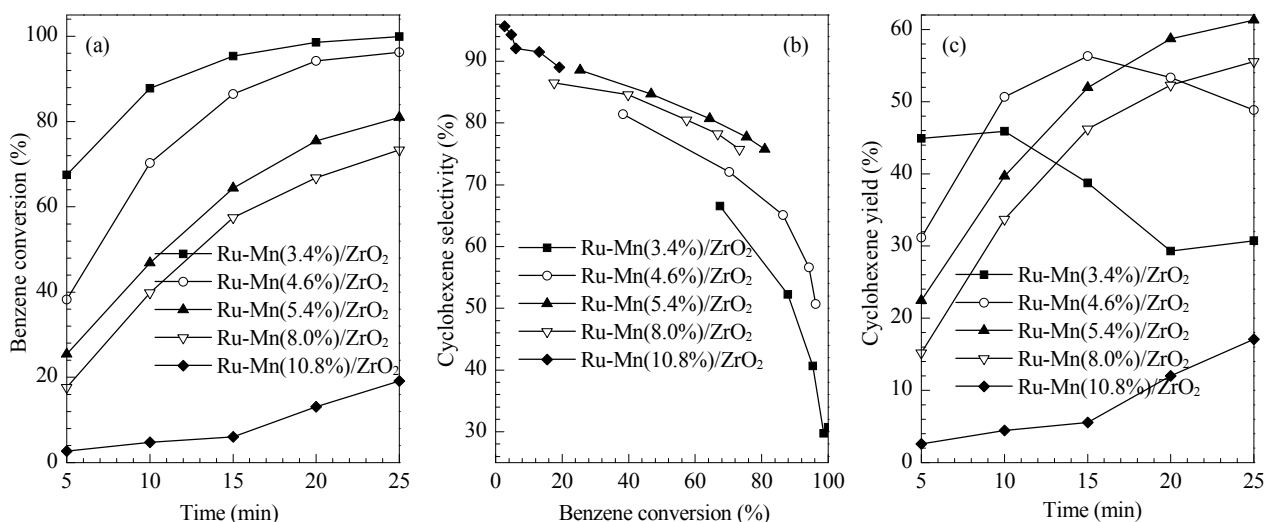


Fig. 4. Performance of Ru-Mn(x)/ZrO₂ catalysts with different Mn contents for selective hydrogenation of benzene to cyclohexene. Reaction conditions: a share of Ru-Mn(x) catalyst, 49.2 g ZnSO₄·7H₂O, 9.8 g ZrO₂, 280 ml H₂O, 5 MPa H₂, 150 °C, stirring rate 1400 r/min.

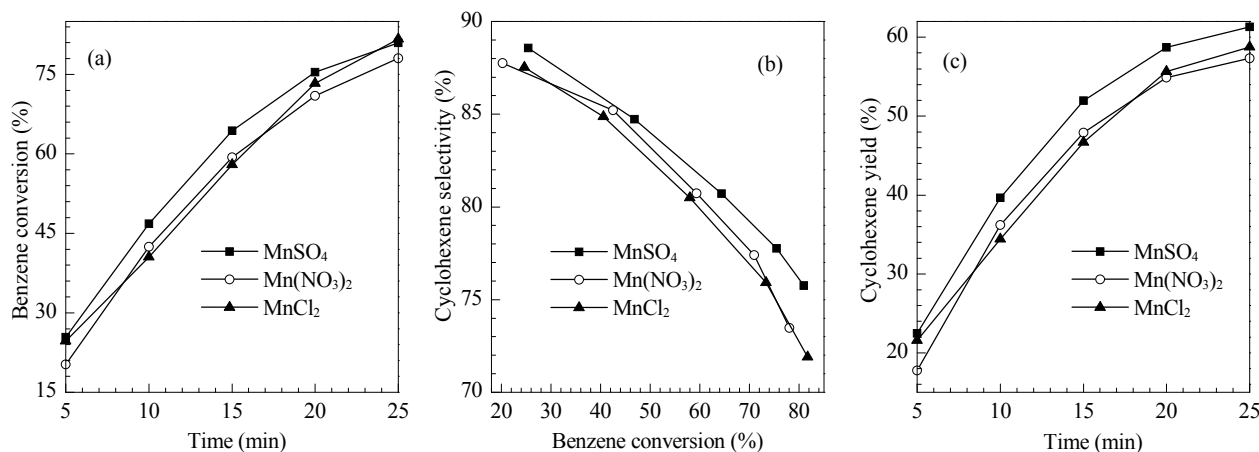


Fig. 5. Performance of Ru-Mn(5.4%)/ZrO₂ catalysts prepared by different Mn precursors. Reaction conditions: a share of Ru-Mn(x) catalyst, 49.2 g ZnSO₄·7H₂O, 9.8 g ZrO₂, 280 ml H₂O, 5 MPa H₂, 150 °C, stirring rate 1400 r/min.

To summarize, the Mn promoter in the Ru-Mn(x) catalysts existed as Mn₃O₄ on the Ru surface. The Mn₃O₄ reacted with ZnSO₄ to form the [Zn(OH)₂]₃(ZnSO₄)(H₂O)₃ salt in the hydrogenation process. This salt could be readily chemisorbed on the Ru surface and directly affected the performance of the Ru catalyst in the selective hydrogenation of benzene to cyclohexene.

3.2. Performances of Ru-Zn(x) catalysts in selective hydrogenation of benzene to cyclohexene

Figure 4 shows the performances of Ru-Mn(x) catalysts with different Mn contents, using ZrO₂ as a dispersant, for the selective hydrogenation of benzene to cyclohexene. As can be seen from Fig. 4(a) and (b), the catalytic activity increased and the cyclohexene selectivity at the same benzene conversion decreased with Mn content of the catalyst. Obviously, the increase in cyclohexene selectivity was achieved at the expense of catalytic activity. As can be seen from Fig. 4(c), the cyclohexene yields continuously increased when the Mn content of the catalyst increased from 3.4% to 5.4%. However, with further increases in the Mn content, the cyclohexene yields increased gradually. The Ru-Mn(5.4%) catalyst gave a cyclohexene yield of 61.3%, which is among the best results reported so far [9,29]. It should also be noted that the Ru-Mn(5.4%) catalyst without ZrO₂ gave a cyclohexene selectivity of 82.7% at a benzene conversion of 59.4% at 15 min. The activity was lower (64.4%) and the cyclohexene selectivity was slightly higher (80.7%) than those with ZrO₂. This implied that the ZrO₂ played an important role in dispersing the Ru catalyst particles; this is consistent with the TEM results.

The results described above show that the amount of [Zn(OH)₂]₃(ZnSO₄)(H₂O)₃ salt formed in the hydrogenation process increased with the Mn₃O₄ content of the Ru-Mn(x) catalysts. The chemisorbed [Zn(OH)₂]₃(ZnSO₄)(H₂O)₃ salt played a key role in improving the cyclohexene selectivity of the Ru catalyst. (1) The chemisorbed [Zn(OH)₂]₃(ZnSO₄)(H₂O)₃ salt was rich in crystallization water. Chemisorption of the salt on the surface of the catalyst therefore resulted in the Ru catalyst being surrounded by a stagnant water layer. The existence of a stagnant water layer on the catalyst surface could accelerate

desorption and hinder re-adsorption of cyclohexene for further hydrogenation to cyclohexane [13,30]. (2) The Zn²⁺ of the chemisorbed [Zn(OH)₂]₃(ZnSO₄)(H₂O)₃ salt could selectively cover most reactive sites of the catalyst, which could reduce the adsorption enthalpies of cyclohexene and benzene. A decrease in the adsorption enthalpy of cyclohexene could result in an increase in the cyclohexene desorption rate, and hence an increase in the cyclohexene selectivity. However, a decrease in the adsorption enthalpy of benzene would lead to a decrease in the catalytic activity [24,30]. (3) Electronic interactions between Zn²⁺ of the chemisorbed [Zn(OH)₂]₃(ZnSO₄)(H₂O)₃ salt and the active Ru components could modify the electronic structure of Ru, which might be favorable for the formation of cyclohexene [13,20,30]. (3) The Zn²⁺ of the chemisorbed [Zn(OH)₂]₃(ZnSO₄)(H₂O)₃ salt could form loosely bound adducts with cyclohexene, which could stabilize the cyclohexene formed on the surface of the Ru catalyst and improve the cyclohexene selectivity [9,20,29]. The activities of the Ru-Mn(x) catalysts therefore decreased and the cyclohexene selectivities increased with increasing amounts of chemisorbed [Zn(OH)₂]₃(ZnSO₄)(H₂O)₃ salt. The [Zn(OH)₂]₃(ZnSO₄)(H₂O)₃

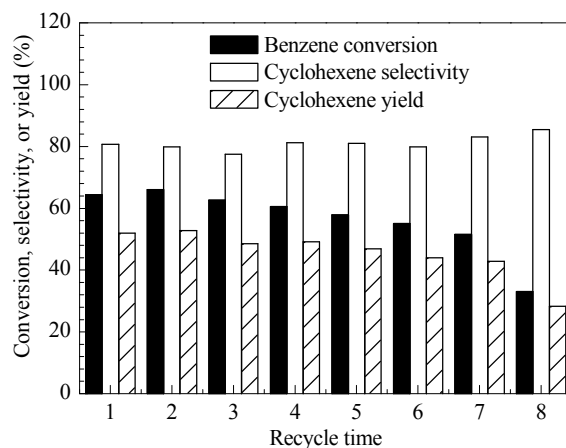
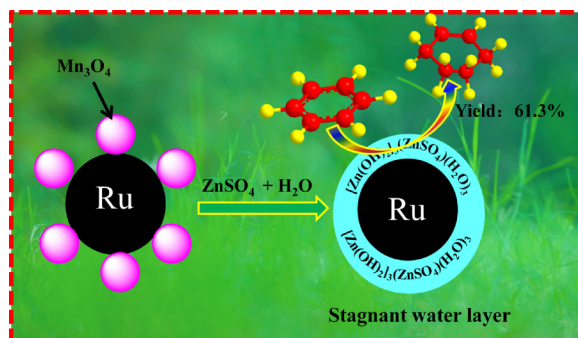


Fig. 6. Reusability of the Ru-Mn(5.4%)/ZrO₂ catalyst for selective hydrogenation of benzene to cyclohexene. Reaction conditions: a share of Ru-Mn(x) catalyst, 49.2 g ZnSO₄·7H₂O, 9.8 g ZrO₂, 280 ml H₂O, 5 MPa H₂, 150 °C, stirring rate 1400 r/min.

Graphical Abstract

Chin. J. Catal., 2013, 34: 684–694 doi: 10.1016/S1872-2067(11)60489-0

Selective hydrogenation of benzene to cyclohexene over nanocomposite Ru-Mn/ZrO₂ catalystsSUN Haijie, JIANG Houbing, LI Shuaihui, WANG Hongxia, PAN Yajie, DONG Yingying, LIU Shouchang, LIU Zhongyi*
Zhengzhou University

An Ru-Mn catalyst with an optimum Mn content of 5.4% gave a cyclohexene yield of 61.3%. The chemisorbed [Zn(OH)₂]₃(ZnSO₄)(H₂O)₃ salt, which was formed by the reaction of Mn₃O₄ with ZnSO₄ in the slurry, improved the selectivity of the Ru catalyst.

salt chemisorbed on the Ru surface therefore played a decisive role in the enhancement of the cyclohexene selectivities of the Ru catalysts.

Figure 5 shows the performances of the Ru-Mn(*x*) catalysts prepared using different precursors, with ZrO₂ as a dispersant, for selective hydrogenation of benzene to cyclohexene. As can be seen, the activities, the cyclohexene selectivities, and the cyclohexene yields of these catalysts were all very similar. The characterization results confirmed that these catalysts had similar chemical compositions. This could be responsible for the very similar performances of these catalysts. The results also suggest that the SO₄²⁻, NO₃⁻, and Cl⁻ ions of the Mn precursors had little effect on the performances of these catalysts.

Figure 6 shows the reusability of the Ru-Mn(5.4%) catalyst with ZrO₂. As can be seen, benzene conversion and cyclohexene selectivity were stable, at above 60.6% and 77.5%, respectively, and the cyclohexene yields remained above 48.5% in the first four cycles. From the fifth cycle to the seventh cycle, the benzene conversion gradually decreased. However, benzene conversion was still above 50%, and the cyclohexene selectivities and yields remained above 80% and 40%, respectively. This indicates that Ru-Mn(5.4%)/ZrO₂ had good stability and potential for industrial applications. The benzene conversion declined drastically to 33.1% in the eighth cycle. However, the cyclohexene selectivity remained as high as 85.4%. The main reasons for the deactivation of the catalyst were the loss of catalyst and the absence of regeneration for long recycling times. Sulfur and nitrogen poisoning might also deactivate the catalyst [31].

4. Conclusions

That Mn in Ru-Mn(*x*) catalysts existed as Mn₃O₄ on the Ru surface. The Mn₃O₄ could react with ZnSO₄ in the slurry to form a [Zn(OH)₂]₃(ZnSO₄)(H₂O)₃ salt. The [Zn(OH)₂]₃(ZnSO₄)(H₂O)₃

salt chemisorbed on the Ru surface played a key role in improving the cyclohexene selectivity of the Ru catalyst. These results indicate that some catalyst promoters could react with additives to form new substances. These new substances might significantly affect the selectivity and activity of the catalyst. This might provide new ideas for understanding the action mechanism of promoters in catalysis.

References

- [1] Zhou X L, Sun H J, Guo W, Liu Zh Y, Liu Sh Ch. *J Nat Gas Chem*, 2011, 20: 53
- [2] Wang W T, Liu H Zh, Wu T B, Zhang P, Ding G D, Liang Sh G, Jiang T, Han B X. *J Mol Catal A*, 2012, 355: 174
- [3] Wang L J, Zhang A Q, Li L, Liu H F, Liu Sh Zh. *Acta Chim Sin*, 2012, 70: 1021
- [4] Qin Y F, Xue W, Li F, Wang Y J, Wei J F. *Chin J Catal*, 2011, 32: 1727
- [5] Sun H J, Guo W, Zhou X L, Chen Zh H, Liu Zh Y, Liu Sh Ch. *Chin J Catal*, 2011, 32: 1
- [6] Xie S H, Qiao M H, Li H X, Wang W J, Deng J F. *Appl Catal A*, 1999, 176: 129
- [7] Liu Sh Ch, Liu Zh Y, Wang Zh, Wu Y M, Yuan P. *Chem Eng J*, 2008, 139: 157
- [8] Fan G Y, Jiang W D, Wang J B, Li R X, Chen H, Li X J. *Catal Commun*, 2008, 10: 98
- [9] Liu J L, Zhu L J, Pei Y, Zhang J H, Li H, Li H X, Qiao M H, Fan K N. *Appl Catal A*, 2009, 353: 282
- [10] Liu Sh Ch, Liu Zh Y, Wang Zh, Zhao Sh H, Wu Y M. *Appl Catal A*, 2006, 313: 49
- [11] Sun H J, Zhang Ch, Yuan P, Li J X, Liu Sh Ch. *Chin J Catal*, 2008, 29: 441
- [12] Liu Zh Y, Sun H J, Wang D B, Liu Sh Ch, Li Zh J. *Chin J Chem*, 2010, 28: 1927
- [13] Sun H J, Zhang X D, Chen Zh H, Zhou X L, Guo W, Liu Zh Y, Liu Sh Ch. *Chin J Catal*, 2011, 32: 224
- [14] Liu Zh Y, Liu Sh Ch, Sun H J, Yuan X M, Yang K J, Zheng R, Wang M J, Li X X, Chen Zh H, Dong Y Y, Wang H X, Pan Y J, Li Sh H. CN Patent

- 102 600 841 A. 2012
- [15] Morales F, de Groot F M F, Glatzel P, Kleimeov E, Bluhm H, Hävecker M, Knop-Gericke A, Weckhuysen B M. *J Phys Chem B*, 2004, 108: 16201
- [16] Xie Y Ch, Wang Ch B, Tang Y Q. *Sci China (Ser B)*, 1993, 23: 113
- [17] Nagahara H, Konishi M. US Patent 4 734 536. 1988
- [18] Zhang Y P, Wang X L, Shen K, Xu H T, Sun K Q, Zhou Ch Ch. *Chin J Catal*, 2012, 33: 1523
- [19] Sun H J, Pan Y J, Wang H X, Dong Y Y, Liu Zh Y, Liu Sh Ch. *Chin J Catal*, 2012, 33: 610
- [20] Wang J Q, Wang Y Zh, Xie S H, Qiao M H, Li H X, Fan K N. *Appl Catal A*, 2004, 272: 29
- [21] Yuan P Q, Wang B Q, Ma Y M, He H M, Cheng Zh M, Yuan W K. *J Mol Catal A*, 2009, 301: 140
- [22] He H M, Yuan P Q, Ma Y M, Cheng Zh M, Yuan W K. *Chin J Catal*, 2009, 30: 312
- [23] Sun H J, Chen Zh H, Guo W, Zhou X L, Liu Zh Y, Liu Sh Ch. *Chin J Chem*, 2011, 29: 369
- [24] Struijk J, Moene R, van der Kamp T, Scholten J J F. *Appl Catal A*, 1992, 89: 77
- [25] Peplinski B, Unger W E S, Grohmann I. *Appl Surf Sci*, 1992, 62: 115
- [26] Dai W L, Sun Q, Deng J F, Wu D, Sun Y H. *Appl Surf Sci*, 2001, 177: 172
- [27] Silvestre-Albero J, Serrano-Ruiz J C, Sepúlveda-Escribano A, Rodríguez-Reinoso F. *Appl Catal A*, 2005, 292: 244
- [28] Ramos-Fernández E V, Ferreira A F P, Sepúlveda-Escribano A, Kapteijn F, Rodríguez-Reinoso F. *J Catal*, 2008, 258: 52
- [29] Liu J L, Zhu Y, Liu J, Pei Y, Li Zh H, Li H, Li H X, Qiao M H, Fan K N. *J Catal*, 2009, 268: 100
- [30] Sun H J, Wang H X, Jiang H B, Li S H, Liu S C, Liu Z Y, Yuan X M, Yang K L. *Appl Catal A*, 2013, 450: 160
- [31] Wu J M, Yang Y F, Chen J L. *Chem Ind Eng Progr*, 2003, 22: 295